JACC: CARDIOVASCULAR IMAGING VOL. ■, NO. ■, 2021

Right Ventricular Functional Abnormalities in Arrhythmogenic Cardiomyopathy

Association With Life-Threatening Ventricular Arrhythmias

Feddo P. Kirkels, MD,[a,b,c] Øyvind H. Lie, MD, PhD,[b,c] Maarten J. Cramer, MD, PhD,[a] Monica Chivulescu, MD,[b,c] Christine Rootwelt-Norberg, MD,[b,c] Folkert W. Asselbergs, MD, PhD,[a,d,e] Arco J. Teske, MD, PhD,[a] Kristina H. Haugaa, MD, PhD[b,c]

ABSTRACT

OBJECTIVES This study aimed to perform an external validation of the value of right ventricular (RV) deformation patterns and RV mechanical dispersion in patients with arrhythmogenic cardiomyopathy (AC). Secondly, this study assessed the association of these parameters with life-threatening ventricular arrhythmia (VA).

BACKGROUND Subtle RV dysfunction assessed by echocardiographic deformation imaging is valuable in AC diagnosis and risk prediction. Two different methods have emerged, the RV deformation pattern recognition and RV mechanical dispersion, but these have neither been externally validated nor compared.

METHODS We analyzed AC probands and mutation-positive family members, matched from 2 large European referral centers. We performed speckle tracking echocardiography, whereby we classified the subtricuspid deformation patterns from normal to abnormal and assessed RV mechanical dispersion from 6 segments. We defined VA as sustained ventricular tachycardia, appropriate implantable cardioverter-defibrillator therapy, or aborted cardiac arrest.

RESULTS We included 160 subjects, 80 from each center (43% proband, 55% women, age 41 ± 17 years). VA had occurred in 47 (29%) subjects. In both cohorts, patients with a history of VA showed abnormal deformation patterns (96% and 100%) and had greater RV mechanical dispersion (53 ± 30 ms vs. 30 ± 21 ms; $p < 0.001$ for the total cohort). Both parameters were independently associated to VA (adjusted odds ratio: 2.71 [95% confidence interval: 1.47 to 5.00] per class step-up, and 1.26 [95% confidence interval: 1.07 to 1.49]/10 ms, respectively). The association with VA significantly improved when adding RV mechanical dispersion to pattern recognition (net reclassification improvement 0.42; $p = 0.02$ and integrated diagnostic improvement 0.06; $p = 0.01$).

CONCLUSIONS We externally validated 2 RV dysfunction parameters in AC. Adding RV mechanical dispersion to RV deformation patterns significantly improved the association with life-threatening VA, indicating incremental value. (J Am Coll Cardiol Img 2021;■:■–■) © 2021 The Authors. Published by Elsevier on behalf of the American College of Cardiology Foundation. This is an open access article under the CC BY-NC-ND license (http://creativecommons.org/licenses/by-nc-nd/4.0/).

From the [a]Department of Cardiology, Division Heart and Lungs, University Medical Center Utrecht, Utrecht, the Netherlands; [b]Department of Cardiology, Oslo University Hospital, Rikshospitalet, Oslo, Norway; [c]Institute of Clinical Medicine, Faculty of Medicine, University of Oslo, Oslo, Norway; [d]Utrecht University, Utrecht, the Netherlands; and the [e]Institute of Cardiovascular Science and Institute of Health Informatics, Faculty of Population Health Sciences, University College London, London, United Kingdom.

The authors attest they are in compliance with human studies committees and animal welfare regulations of the authors' institutions and Food and Drug Administration guidelines, including patient consent where appropriate. For more information, visit the Author Center.

Manuscript received September 8, 2020; revised manuscript received December 16, 2020, accepted December 17, 2020.

ISSN 1936-878X https://doi.org/10.1016/j.jcmg.2020.12.028

ABBREVIATIONS AND ACRONYMS

AC = arrhythmogenic cardiomyopathy

AUC = area under the curve

CMR = cardiac magnetic resonance

ECG = electrocardiogram

ICD = implantable cardioverter-defibrillator

RV = right ventricle

TFC = Task Force Criteria

VA = life-threatening ventricular arrhythmia

Arrhythmogenic cardiomyopathy (AC) (also known as arrhythmogenic right ventricular cardiomyopathy) is an inheritable cardiomyopathy, characterized by life-threatening ventricular arrhythmias (VA) and progressive cardiac failure (1). In the classic phenotype, pathogenic mutations encoding for desmosomal proteins lead to primarily right ventricular (RV) myocyte loss and replacement by fibrofatty tissue (2,3).

Already in the early stage of the disease, life-threatening arrhythmias can occur, making it a leading cause of sudden cardiac death amongst young, seemingly healthy individuals (2–4). Early detection of the disease is thus of great importance. Currently, AC is diagnosed according to a complex set of criteria, defined in the 2010 revised Task Force Criteria (TFC), in which cardiac imaging has an important role (5).

In addition to conventional imaging parameters, as incorporated in the 2010 TFC, echocardiographic deformation imaging has been described for detection of subtle phenotypic expressions in early AC as well as for risk prediction regarding ventricular arrhythmias (6–11). The technique has been applied to the RV in patients with AC in different ways: by recognition of deformation patterns of the RV subtricuspid area (6,7), and by using the mechanical dispersion, a measure of heterogeneous contraction, as a parameter of disease expression (8–10). These 2 methods have successfully been tested in separate cohorts of the centers where they were developed, but are not yet implemented in clinical care outside of these centers. To advance RV deformation imaging closer to standard clinical care in AC, it is pivotal to show that these results are not only achieved in 1 center. To date, the value of RV deformation patterns and mechanical dispersion has never been externally validated. Furthermore, the association between RV deformation patterns and ventricular arrhythmias has not been investigated previously, and it is not known whether the 2 methods measure essentially the same phenomenon or if combining the 2 methods adds value to risk stratification of VA.

We aimed to perform an external validation of the association between RV deformation patterns and disease stage in AC. Furthermore, we aimed to validate mechanical dispersion as a marker of ventricular arrhythmias. Finally, we wanted to explore the added value of combining the parameters.

METHODS

STUDY DESIGN AND POPULATION. This study was conducted in 2 academic referral centers for AC in Europe. We used an AC cohort from the University Medical Center Utrecht in the Netherlands and an age- and sex-matched AC cohort from the Oslo University Hospital in Norway. Probands underwent genetic testing as described previously (12), and cascade genetic screening was performed in family members of genotype positive probands. The Utrecht cohort consisted of 80 AC probands and genotype-positive family members with an echocardiographic examination including RV deformation imaging in Utrecht between 2006 and 2015, who have been reported previously (6). During this period, 87 subjects were evaluated, of which 7 were excluded due to inadequate image quality for RV deformation analyses. The Oslo cohort also consisted of 80 AC probands and genotype positive family members. By matching to the Utrecht subjects based on age and sex, the Oslo subjects were selected from a previously reported cohort of 144 subjects who were referred between 1997 and 2016 (13). Due to inadequate image quality for RV deformation analyses, 4 subjects were replaced by other matched subjects from the Oslo cohort during the matching process. For the purpose of external validation, the 2 cohorts were kept separated first. The association between RV deformation patterns and disease stage was determined in the Oslo cohort and compared to the Utrecht cohort, where the method was initially developed. The external validity of the association between RV mechanical dispersion and arrhythmic events was tested in the Utrecht cohort and compared to the Oslo cohort. Subsequently, the 2 cohorts were merged to compare both RV deformation techniques and to explore the added value of combining them in the total cohort. The study was approved by both local institutional ethics review boards and complies with the Declaration of Helsinki.

DATA COLLECTION. We recorded clinical characteristics at inclusion, including demographics, antiarrhythmic or beta-blocker medication, presence of an implantable cardioverter-defibrillator (ICD), and history of cardiac syncope (sudden loss of consciousness followed by spontaneous sudden awakening). By applying the 2010 TFC (5), we determined fulfillment of a definite AC diagnosis. Date of inclusion was defined as the date of first complete echocardiographic examination suitable for performing deformation imaging.

Electrocardiography. We performed standard 12-lead electrocardiogram (ECG) recording and 24-h Holter monitoring at inclusion. The extent of T-wave inversions, presence of epsilon waves, and increased terminal activation duration were recorded according

FIGURE 1 **Echocardiographic Deformation Imaging of the RV**

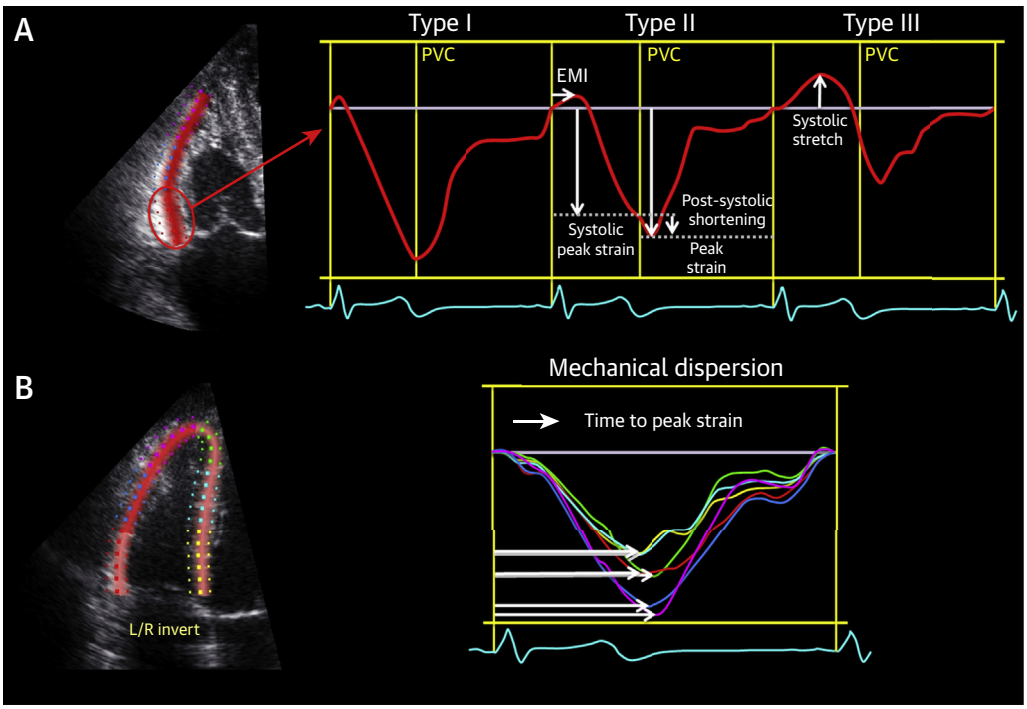

Right ventricular (RV) deformation pattern recognition of the basal segment and RV mechanical dispersion performed on an RV-focused 4-chamber view. **(A)** Based on predefined criteria, a division into 3 different deformation patterns is identified (6). Type I is normal deformation; type II is characterized by delayed onset of shortening, reduced systolic peak strain, and minor post-systolic shortening; type III is characterized by little or no systolic peak strain, predominantly systolic stretching, and major post-systolic shortening. **(B)** For right ventricular mechanical dispersion (RVMD), a 6-segment model of the RV was used, including both the lateral wall and the interventricular septum. It was calculated as the SD of the segmental time intervals from onset Q/R on the surface ECG to peak negative strain and expressed in ms (8,9). **Horizontal arrows in B** indicate the time interval until peak shortening for each segment. EMI = electromechanical interval (time to onset of shortening); PVC = pulmonic valve closure.

to the 2010 TFC. Arrhythmias were recorded on 12-lead ECG, Holter, or ICD monitoring (5). The amount of premature ventricular complexes per 24 h on Holter monitoring was documented, and nonsustained ventricular tachycardia was defined as consecutive runs of ≥3 ventricular beats >100 beats/min for <30 s (14).

Echocardiography. We performed echocardiography, using a GE Vivid 7, E9 or E95 scanner (GE Healthcare, Horten, Norway). Cine loops were stored for post-processing with EchoPac version 202 (GE Healthcare). We assessed structural and functional abnormalities defined in the 2010 TFC (5) and parameters from the EACVI consensus paper (15).

Details on acquisition of the RV-focused 4-chamber view and post-processing in echocardiographic speckle tracking deformation imaging were previously described more extensively (16–18). We assessed the subtricuspid deformation pattern in a single wall tracing of the RV lateral free wall, which was automatically divided into a basal, mid, and apical segment. Timing of the pulmonary valve closure was assessed by Doppler traces in the RV outflow tract, obtained in the parasternal short-axis view. The following deformation parameters were measured in the basal segment: time to onset of shortening (or electromechanical interval) (19), systolic peak strain (20), and the amount post-systolic shortening (21) (definitions in Supplemental Appendix). Based on these parameters, a distinction into 3 different deformation patterns has previously been observed in AC and simulated using a computer model (6) (**Figure 1A**). For RV mechanical dispersion, we used a 6-segment RV model, including both the lateral wall and the interventricular septum. It was calculated as the SD of the segmental time intervals from onset Q/R on the surface ECG to maximum shortening, represented by the automatically

detected peak negative strain (8,9) (**Figure 1B**). The left ventricular global longitudinal strain (GLS) was calculated in a 16-segment left ventricular model (22-24). RV free-wall longitudinal strain was calculated as the averaged peak systolic strain from 3 RV free-wall segments. All measurements were performed by a single observer blinded to clinical outcome, who was newly trained in both RV deformation imaging techniques and was not involved in the initial development of the methods. Intraobserver and interobserver variability of deformation imaging parameters was assessed by reanalyzing 20 echocardiographic studies in both the Utrecht and Oslo databases (Supplemental Appendix).

Cardiac magnetic resonance. Cardiac magnetic resonance (CMR) imaging was performed on a 1.5-T scanner, as published previously and according to standard AC protocols (6,12). Available data were analyzed for structural abnormalities fulfilling 2010 TFC (5). Conventional CMR measurements included RV end-diastolic volume indexed for body surface area and RV ejection fraction (RVEF). Contrast-enhanced images with administration of gadolinium were acquired for detection of myocardial fibrosis in both ventricles, presenting as late gadolinium enhancement.

OUTCOMES. All arrhythmic events were adjudicated retrospectively from the time of echocardiographic assessment. Life-threatening ventricular arrhythmia was defined as a documented history of sustained ventricular tachycardia, aborted cardiac arrest, or appropriate ICD therapy. The division into 3 different disease stages was based on the presence of subsets of the 2010 TFC, as described previously (5,6). In brief, subjects in the *structural* stage presented with minor or major 2010 TFC for structural abnormalities on echocardiography or CMR. Subjects categorized in the *electrical* stage fulfilled no structural criteria but had minor or major ECG abnormalities (repolarization and/or depolarization) and/or history of ventricular arrhythmias as defined by the 2010 TFC. *Subclinical* subjects were defined as fulfilling neither structural, nor electrical 2010 TFC.

STATISTICAL ANALYSIS. Analyses were performed with SPSS statistics for Windows 21 (IBM, Armonk, New York) and Stata/SE version 16.0 (StataCorp, College Station, Texas). Continuous data were presented as mean ± SD and categorical variables were presented as frequencies (percentage of cases). Continuous variables were compared by independent Student's *t*-tests and categorical data by chi-square or Fisher exact tests. The association to VA was assessed by the area under the receiver-operating characteristics curve (AUC). Odds ratios and 95% confidence intervals were calculated for RV deformation patterns and mechanical dispersion using univariable and multivariable logistic regression. The incremental value of combining RV deformation patterns with mechanical dispersion was assessed by reclassification analysis by integrated diagnostic improvement and continuous net reclassification improvement, and the AUCs of different models were compared. Mechanical dispersion was dichotomized at an optimal cutoff derived from a single threshold regression analysis. This threshold was defined as the point estimate that best classified 2 groups with the most diverging odds ratios. Intraobserver and interobserver variability was expressed by kappa statistics or intraclass correlation coefficient, as appropriate. All p values were 2-sided, and p values < 0.05 were considered significant.

RESULTS

CLINICAL CHARACTERISTICS. We included 160 patients (55% women, age 41 ± 17 years), comprising 68 probands and 92 mutation-positive family members, from 86 different families. Plakophilin-2 was the most common pathogenic mutation in both the Oslo and Utrecht cohort (90% and 89%, respectively). Most probands (n = 55 [81%]) and part of the family members (n = 42 [46%]) fulfilled a definite 2010 TFC AC diagnosis (5). Life-threatening ventricular arrhythmia had occurred in 47 (29%) of the subjects, with similar rates in the Oslo and Utrecht cohort (25 [31%] vs. 22 [28%]; p = 0.60): documented sustained ventricular tachycardia in 37, aborted cardiac arrest in 8, and appropriate ICD therapy in 2. More patients from the Oslo cohort were categorized in the electrical disease stage (25 [31%] vs. 13 [16%]; p = 0.03), whereas the other disease stages were equally represented in both cohorts (**Table 1**).

VENTRICULAR ARRHYTHMIAS. Patients with VA were predominantly men (n = 28; 60%) and were significantly older (46.4 ± 13.9 years vs. 38.2 ± 16.8 years; p = 0.002). Only 2 (2%) of the mutation-positive family members had experienced the arrhythmic outcome at evaluation (**Table 2**) (analyses separated by center are displayed in the Supplemental Tables 1 to 3). Patients with VA had worse conventional echocardiographic parameters at inclusion, except for left ventricular EF (**Table 3**).

RV subtricuspid deformation patterns were similarly distributed within the 2 cohorts (**Figure 2A**) and were more abnormal in patients with VA. Among VA patients, 46 (98%) had an abnormal RV deformation pattern type II (n = 16 [34%]) or type III (n = 30 [64%]).

Odds for VA significantly increased with each step-up in type (OR: 3.91 [95% CI: 2.23 to 6.85]; $p < 0.001$), also when adjusted for age at outcome adjudication (OR: 3.55 [95% CI: 1.97 to 6.42]; $p < 0.001$).

Patients with VA had more pronounced RV mechanical dispersion (53 ± 30 ms vs. 30 ± 21 ms; $p < 0.001$). This difference was evident in both cohorts (45 ± 25 ms vs. 26 ± 15 ms; $p < 0.001$ in the Oslo cohort and 63 ± 33 ms vs. 34 ± 25 ms; $p < 0.001$ in the Utrecht cohort) (Figure 2B). Every 10-ms increase in RV mechanical dispersion increased the odds of observing VA by 45% (OR: 1.45 [95% CI: 1.23 to 1.71]; $p < 0.001$). When adjusted for age, the increased odds was comparable (OR: 1.41 [95% CI: 1.18 to 1.69]; $p < 0.001$). The optimal cutoff for RV mechanical dispersion to detect patients with a history of VA was 24 ms (OR: 1.06 [95% CI: 0.96 to 1.18]/10-ms increment <24 ms and 1.57 [95% CI: 1.45 to 1.71]/10-ms increment >24 ms).

The AUC significantly decreased when dichotomizing RV mechanical dispersion, compared with using it as a continuous variable (0.71 [95% CI: 0.64 to 0.77] vs. 0.78 [95% CI: 0.71 to 0.86]; $p = 0.01$). Therefore, RV mechanical dispersion was used only as a continuous variable.

ROC analysis showed a reasonable association between deformation pattern recognition and VA (AUC 0.74 [95% CI: 0.66 to 0.82]) and between RV mechanical dispersion and VA (AUC 0.78 [95% CI: 0.71 to 0.86]), when used separately. We observed no difference between the associations in the Oslo and Utrecht cohort for both pattern recognition (AUC 0.77 [95% CI: 0.68 to 0.86] vs. 0.72 [95% CI: 0.61 to 0.83]; $p = 0.49$), and RV mechanical dispersion (AUC 0.76 [95% CI: 0.65 to 0.88] vs. 0.81 [95% CI: 0.72 to 0.91]; $p = 0.50$).

All deformation analyses showed excellent intra- and inter-observer agreement (Supplemental Table 4).

COMBINING THE 2 RV DEFORMATION METHODS. RV deformation patterns and RV mechanical dispersion were partially concordant, but also independently associated with VA (adjusted OR: 2.71 [95% CI: 1.47 to 5.00] per step-up and 1.26 [95% CI: 1.07 to 1.49]/10-ms increment, respectively). Patients with abnormal deformation patterns (type II or III) had increased odds for VA (OR: 27.21 [95% CI: 3.62 to 204.63]), and within this subgroup, odds for VA increased by 30% for each 10-ms increase in RV mechanical dispersion (OR: 1.30 [95% CI: 1.11 to 1.53]/10-ms increase). (Central Illustration)

When applying the RV mechanical dispersion in the group with normal or type II deformation patterns, the odds of VA increased by approximately 45% for each 10-ms increase in dispersion (OR: 1.46 [95% CI: 1.08 to 1.96]). Classification significantly improved when adding RV mechanical dispersion to

TABLE 1 Clinical Characteristics and Comparison per Center

	All (N = 160)	Oslo (n = 80)	Utrecht (n = 80)	p Value
Age, yrs	40.6 ± 16.8	40.9 ± 16.1	40.4 ± 17.6	0.87
Female	88 (55)	44 (55)	44 (55)	1.00
Probands	68 (43)	40 (50)	28 (35)	0.06
BSA, m^2	1.9 ± 0.2	1.9 ± 0.2	1.9 ± 0.2	0.31
Definite AC	97 (61)	47 (59)	50 (63)	0.63
AA medication	44 (28)	12 (15)	32 (40)	<0.001
Beta-blockers	60 (38)	27 (34)	33 (41)	0.33
Mutation	139 (87)	59 (75)	80 (100)	<0.001
PKP2	124 (78)	53 (67)	71 (89)	0.001
ICD	20 (14)	7 (9)	13 (19)	0.07
Syncope	40 (25)	30 (38)	10 (13)	<0.001
VA	47 (29)	25 (31)	22 (28)	0.60
Disease stage				
Subclinical	36 (23)	15 (19)	21 (26)	0.26
Electrical	38 (24)	25 (31)	13 (16)	0.03
Structural	86 (54)	40 (50)	46 (58)	0.34

Values are mean ± SD or n (%).

AA = antiarrhythmic; AC = arrhythmogenic cardiomyopathy; BSA = body surface area; ICD = implantable cardioverter-defibrillator; PKP2 = plakophillin-2; VA = life-threatening ventricular arrhythmia.

TABLE 2 Clinical Characteristics and Electrocardiographic Parameters of Patients Without and With Life-Threatening Arrhythmia

	All (N = 160)	No VA (n = 113)	VA (n = 47)	p Value
Age, yrs	41 ± 17	38 ± 17	46 ± 14	0.002
Female	88 (55)	69 (61)	19 (40)	0.01
Probands	68 (43)	23 (20)	45 (96)	<0.001
BSA, m^2	1.9 ± 0.2	1.9 ± 0.2	2.0 ± 0.2	<0.001
Definite AC	97 (61)	57 (50)	40 (85)	<0.001
AA medication	44 (28)	16 (14)	28 (60)	<0.001
Beta-blockers	60 (38)	35 (31)	25 (53)	0.008
Mutation	139 (87)	103 (92)	36 (77)	0.008
PKP2	124 (78)	94 (84)	30 (64)	0.005
ICD	20 (14)	2 (2)	18 (44)	<0.001
Syncope	40 (25)	23 (20)	17 (36)	0.04
HR, beats/min	61 ± 12	63 ± 13	56 ± 10	<0.001
TWI major	45 (28)	22 (20)	23 (49)	<0.001
Epsilon wave	13 (8)	5 (5)	8 (17)	0.008
TAD >55 ms	37 (25)	22 (21)	15 (37)	0.04
PVC >500	43 (27)	33 (30)	10 (22)	0.32
Disease stage				
Subclinical	36 (23)	36 (32)	0 (0)	<0.001
Electrical	38 (24)	31 (27)	7 (15)	0.09
Structural	86 (54)	46 (41)	40 (85)	<0.001

Values are mean ± SD or n (%).

PVC = premature ventricular complex; TAD = terminal activation duration; TWI = T-wave inversion; other abbreviations as in Table 1.

TABLE 3 Cardiac Imaging Parameters of Patients Without and With Life-Threatening Arrhythmia

	All	No VA	VA	p Value
Echocardiography	160	113	47	
RVD, mm	41 ± 10	38 ± 7	48 ± 12	<0.001
RVFAC, %	38 ± 11	42 ± 9	29 ± 9	<0.001
RV deformation pattern I	43 (27)	42 (37)	1 (2)	<0.001
RV deformation pattern II	56 (35)	40 (35)	16 (34)	0.87
RV deformation pattern III	61 (38)	31 (27)	30 (64)	<0.001
$RV_{FW}SL$, %	−19.3 ± 7.6	−21.4 ± 6.5	−14.0 ± 7.7	<0.001
Peak systolic strain basal, %	−14 ± 9	−16 ± 9	−8 ± 8	<0.001
Peak systolic strain mid, %	−20 ± 8	−22 ± 7	−14 ± 8	<0.001
Peak systolic strain apical, %	−24 ± 8	−26 ± 7	−20 ± 10	<0.001
RVMD, ms	37 ± 26	30 ± 21	53 ± 30	<0.001
RVOT, mm	35 ± 8	32 ± 6	40 ± 9	<0.001
TAPSE, mm	21 ± 4	22 ± 4	18 ± 5	<0.001
LVEF, %	57 ± 7	57 ± 6	56 ± 9	0.31
GLS, %	−18.1 ± 3.4	−18.7 ± 2.8	−16.7 ± 4.2	0.003
CMR	129	95	34	
RVEF, %	46 ± 13	49 ± 12	37 ± 13	<0.001
RVEDVi, ml	110 ± 41	99 ± 31	148 ± 48	<0.001
LGE	34 (27)	14 (15)	20 (59)	<0.001

Values are n, mean ± SD, or n (%).

CMR = cardiac magnetic resonance; EDVi = end-diastolic volume indexed; EF = ejection fraction; FAC = fractional area change; GLS = global longitudinal strain; LGE = late gadolinium enhancement; LV = left ventricle; MD = mechanical dispersion; RV = right ventricle; RVEDVi = right ventricular end-diastolic volume indexed for body surface area; RVD = right ventricular diameter; RVEF = right ventricular ejection fraction; $RV_{FW}SL$ = right ventricular free wall longitudinal strain; RVOT = right ventricular outflow tract; TAPSE = tricuspid annular plane systolic excursion.

pattern recognition (net reclassification improvement 0.42; p = 0.02 and integrated diagnostic improvement 0.06; p = 0.01). The association increased from AUC 0.74 (95% CI: 0.66 to 0.82) to 0.80 (95% CI: 0.73 to 0.87); p = 0.001 (**Figure 3**). This association was similar to the association between CMR markers and arrhythmia (**Table 4**).

DISCUSSION

This study provides an external validation of the use of RV deformation pattern recognition and RV mechanical dispersion in patients with AC and mutation-positive family members. Both abnormal deformation patterns and prolonged RV mechanical dispersion were independent markers of patients with a history of VA, highlighting the role of deformation analyses in the echocardiographic assessment of patients with AC. *Combining* the 2 parameters increased the association to VA, indicating an independent and incremental value of these techniques, which may help risk stratification of patients with AC.

RV DEFORMATION PATTERNS. This study, for the first time, links abnormal RV deformation patterns to arrhythmic events. Previous studies have focused on the use of RV deformation patterns for early detection of AC disease manifestation and the correlation with clinical disease stages, based on the presence of 2010 TFC (6,19). Subsequently, prognostic value of the patterns was shown for prediction of disease progression, defined as development of new 2010 TFC during follow-up (7), and structural progression on echocardiography (25).

The distribution of deformation patterns over disease stages of increasing severity was similar in both cohorts and in line with previous results (6), and it was therefore considered a successful external validation (**Figure 2A**). We found clearly abnormal deformation patterns in the RV subtricuspid segment in a significant number of subjects without any electrical or structural 2010 TFC, indicating the presence of mechanical dysfunction already in an early stage of the disease (6).

Importantly, abnormal RV deformation patterns had an excellent sensitivity for detection of patients with VA, with a negative predictive value of 0.98. Specificity was suboptimal when taking only past events into account. A prospective setting is, however, needed, because abnormalities now classified as false-positive might be indicators of a risk of future life-threatening arrhythmic events.

RV MECHANICAL DISPERSION. We observed a marked increase in RV mechanical dispersion for patients with VA in both cohorts with no difference by ROC comparison, suggesting mechanical dispersion as an externally valid marker of VA.

Mean RV mechanical dispersion was higher in the Utrecht cohort, partly caused by several outliers (**Figure 2B**). The association between RV mechanical dispersion and arrhythmia was in line with previous reports on patients with early AC disease (12) and exercise-induced arrhythmias (26).

Previous studies and a consensus document on multimodality imaging in AC have suggested cutoffs for RV mechanical dispersion (8,9,15). We observed that dichotomizing at the optimal threshold resulted in a significant loss of information, indicating better abilities of mechanical dispersion used as a continuous parameter.

COMBINING THE 2 RV DEFORMATION METHODS. Previously, it was not clear whether the 2 RV deformation methods assess the same underlying pathology, and comparative data were not available. By applying both methods on the total cohort and associating them to the same definition of arrhythmic outcome, this study was the first to enable a direct comparison. Both RV deformation pattern

recognition and mechanical dispersion were independently associated with VA. Importantly, the classification of patients with a history of VA significantly improved when adding the RV mechanical dispersion to pattern recognition. This implies that the 2 techniques are complementary and may reflect different pro-arrhythmogenic properties of the myocardium. We chose the clinically most intuitive approach to first evaluate the categorical parameter (deformation patterns), and then add the continuous variable (mechanical dispersion). Although deformation patterns and RV mechanical dispersion are both obtained from longitudinal deformation in the same echocardiographic view, there are 2 important reasons for their unique value. First, mechanical dispersion focusses on heterogeneity in global RV contraction, whereas the deformation pattern is considered to reflect focal substrates in 1 segment. The usually less-affected interventricular septum is included in RV mechanical dispersion for a more robust calculation of the SD and to detect globally delayed contraction of the RV lateral wall. Second, patterns include information on both timing and strain amplitude, whereas strain amplitude has no direct influence on mechanical dispersion. The 2 methods, therefore, have independent strengths and weaknesses. The pattern approach is sensitive to subtle abnormalities in the subtricuspid segment, which may be associated with increased arrhythmic risk. In both cohorts, the subtricuspid segment was shown to be first affected in AC, which is in line with previous reports (27). However, prominent involvement of other RV segments has also been reported in AC (28,29), and focusing on 1 segment is accompanied by the risk of missing information. Importantly, whereas the subtricuspid deformation pattern is not able to detect progression to other RV segments, RV mechanical dispersion will increase along with more extensive disease and helps stratification between intermediate and high arrhythmic risk.

CLINICAL IMPLICATIONS. External validation of RV deformation pattern recognition and mechanical dispersion is a crucial step toward including them in routine clinical assessment and in clinical risk stratification in patients with AC. This study was the first attempt to externally validate the value of these methods. For external validation of the combined approach, a third cohort will be needed.

Current risk stratification tools do not include regional and subtle RV function, but only the global RV function from RV ejection fraction by CMR (30). Deformation imaging contributes as a sensitive marker of early structural and functional abnormalities and may improve risk stratification as shown in this study. The overall association with arrhythmia was similar to CMR markers, but the easily available echocardiography has many practical advantages, especially in patients who cannot undergo CMR imaging.

The increasing use of cascade genetic screening will confront clinicians with an expanding group of asymptomatic patients and relatives with an

FIGURE 2 External Validation of Methods

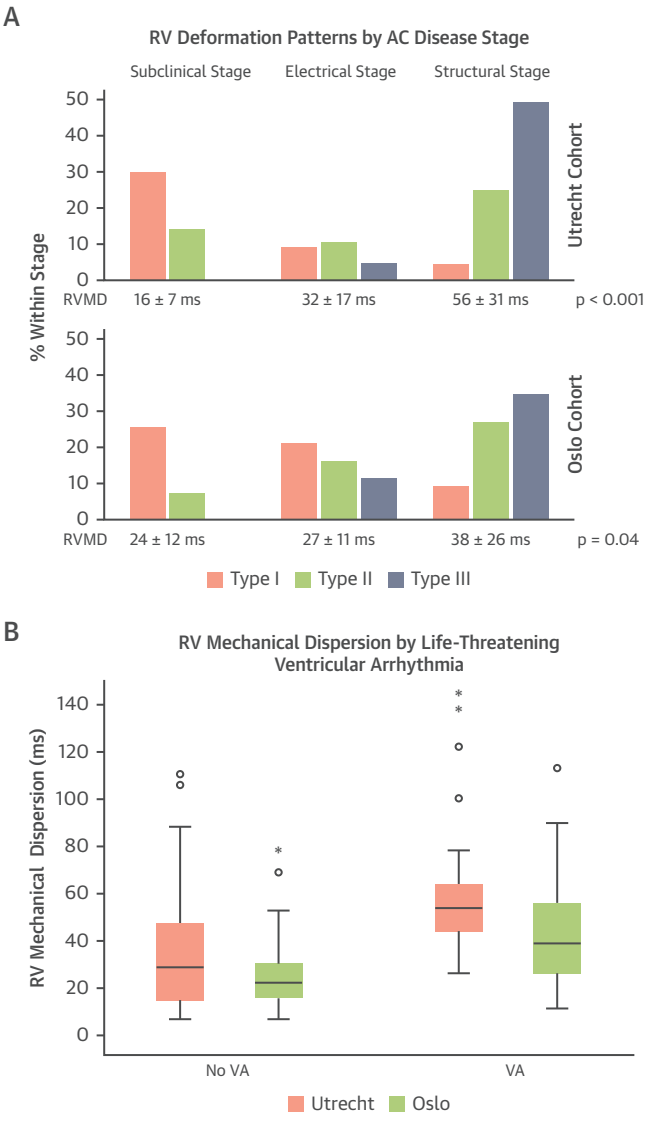

To appreciate the external validity of the RV deformation methods, results are displayed separately for both cohorts. **(A)** Distribution of RV deformation patterns over 3 different diseases. Below each disease stage, the RVMD is reported as mean ± SD. **(B)** Distribution of RV mechanical dispersion for patients with and without a history of life-threatening ventricular arrhythmia (VA). AC = arrhythmogenic cardiomyopathy; RVMD = right ventricular mechanical dispersion.

CENTRAL ILLUSTRATION **Risk Stratification in Arrhythmogenic Cardiomyopathy**

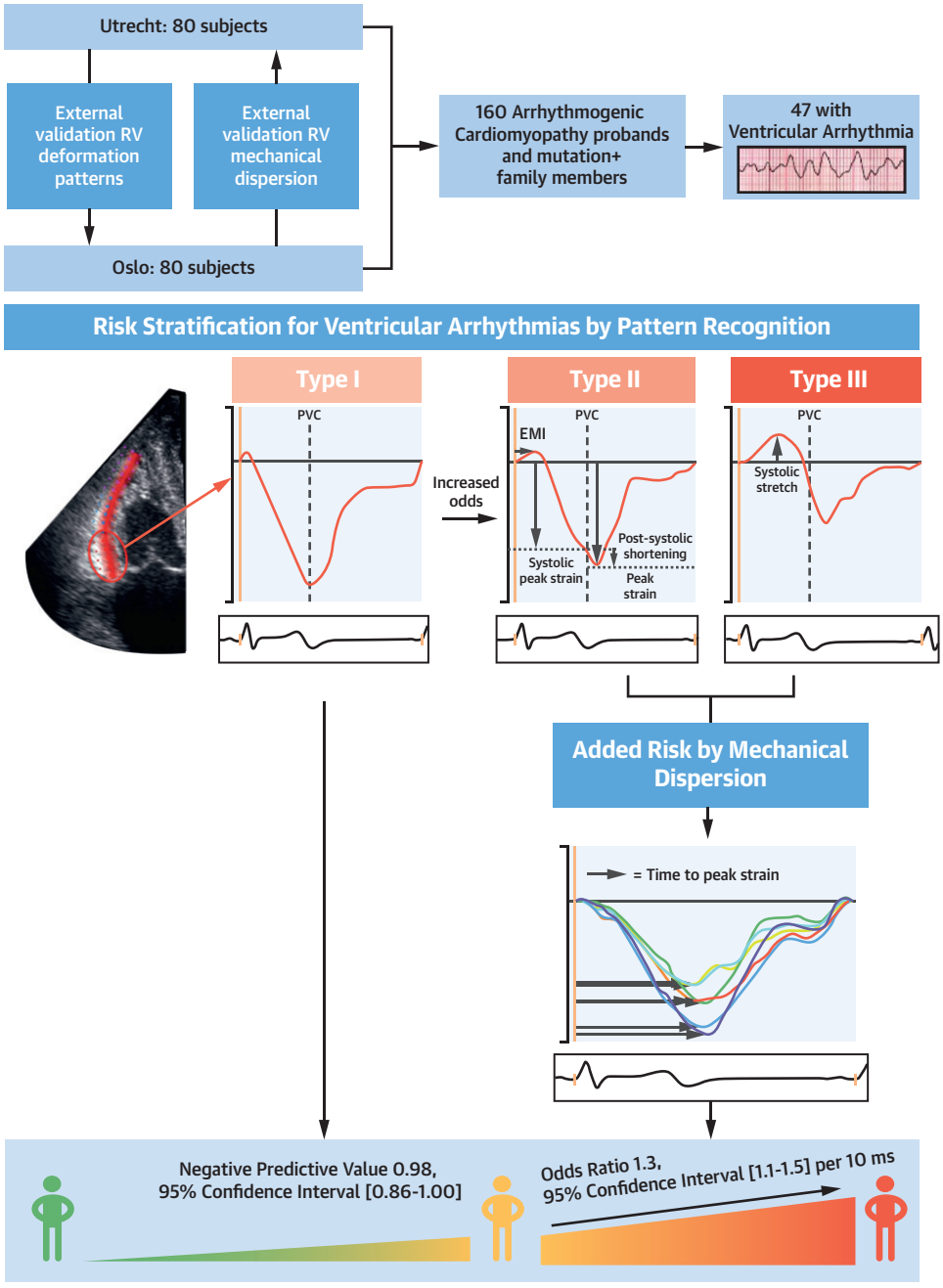

Kirkels, F.P. et al. J Am Coll Cardiol Img. 2021;■(■):■–■.

(Top) We enrolled 160 arrhythmogenic cardiomyopathy probands and mutation-positive family members from 2 large European referral centers, of which 47 had experienced life-threatening ventricular arrhythmias. **(Top Left)** We performed speckle tracking echocardiography, whereby we classified the subtricuspid deformation patterns from normal to abnormal and assessed right ventricular (RV) mechanical dispersion from 6 segments. Both methods were first externally validated and compared with the cohort where the method was developed. **(Bottom Left)** Subsequently, a combined approach was developed, in which a normal deformation pattern (type I) was associated with an excellent negative predictive value, requiring no further analyses. **(Bottom Right)** In patients with an abnormal deformation pattern (type II or III), mechanical dispersion further stratified between intermediate and high arrhythmic risk.

FIGURE 3 Comparison of Models

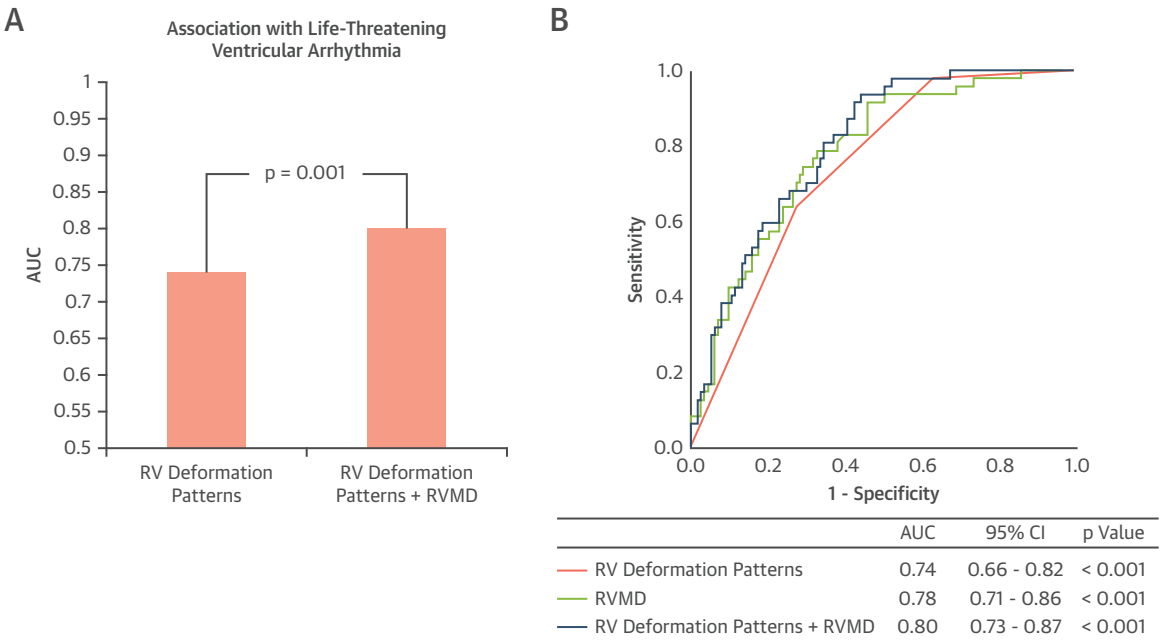

(A) An improved association with life-threatening ventricular arrhythmia was found when combining RV deformation patterns and RVMD, compared with taking only RV deformation patterns into account. This is expressed by an increase in area under the curve (AUC), when comparing receiver-operating curve (ROC) statistics. **(B)** Display of the ROC curves of the individual and combined RV deformation methods. CI = confidence interval; other abbreviations as in Figure 1.

important arrhythmic risk (13). We showed that a normal RV deformation pattern can identify low-risk subjects with excellent negative predictive value. In clinical practice, an initial impression of the deformation pattern can be determined with a brief qualitative determination. Patients with normal deformation patterns would not require quantitative analysis by mechanical dispersion. In patients with borderline abnormal deformation patterns, RV mechanical dispersion may be used for further stratification. In patients with clearly abnormal deformation patterns, a high mechanical dispersion will imply high risk of ventricular arrhythmias. A stepwise approach using both RV deformation indexes is superior as it allows identification of a group of low-risk individuals as well as further arrhythmic risk stratification in others (**Central Illustration**).

STUDY LIMITATIONS. This study had a cross-sectional design with retrospective outcome adjudication with inherent limitations. The predictive value of the investigated parameters should be assessed in a prospective trial. RV deformation imaging reflects partly the same RV functional status as other echocardiographic and CMR indexes, and a multimodality approach will probably offer the best results. To investigate the clinical impact of RV deformation measurements, the additive predictive value should be explored with regard to the existing risk calculation model (30).

A single observer performed all deformation analyses in this study. We considered this a strength for the external validation of the methodology. Although our interobserver variability analysis showed excellent agreement, this approach may represent a limitation for the clinical external validation.

TABLE 4 Association With Arrhythmia of CMR Versus the Combined RV Deformation Imaging Approach

	AUC (95% CI) CMR Marker	Versus RV Deformation Imaging	p Value
RVEF (n = 99)	0.73 (0.61-0.85)	0.74 (0.63-0.84)	0.95
RVEDVi (n = 92)	0.81 (0.69-0.93)	0.77 (0.66-0.87)	0.53
LGE (n = 125)	0.73 (0.63-0.82)	0.76 (0.67-0.84)	0.58

AUC = area under the receiver-operating characteristic curve; CI = confidence interval; CMR = cardiac magnetic resonance; EDVi = end diastolic volume indexed; EF = ejection fraction; LGE = late gadolinium enhancement; RV = right ventricular.

Subjects evaluated at an older age were more likely to have experienced an event. However, also when adjusted for age, RV deformation abnormalities were associated with substantially increased odds for history of VA. Implantation of ICDs caused a risk of bias for detection of arrhythmic events, but due to the low number of appropriate ICD therapies, this risk is considered to be low in the current study.

Data from family members may not be independent. However, because we included patients from 86 different families, we considered it unlikely that overall results were influenced by dependence within single families. A comparison with healthy control subjects was not performed in this study, but can be found for RV deformation patterns (6) and mechanical dispersion (8) separately in previous studies.

The majority of patients had plakophilin-2 mutations, which may limit the extrapolation to other genetic causes of AC.

CONCLUSIONS

This study is the first to externally validate the use of RV deformation pattern recognition and RV mechanical dispersion in AC. RV deformation patterns and mechanical dispersion were independently associated with life-threatening ventricular arrhythmia. Importantly, we observed an added value of combining mechanical dispersion and RV deformation patterns for optimal detection of patients with a history of VA. Future larger prospective studies should investigate the value of combining both parameters in a multimodality risk prediction approach.

ACKNOWLEDGMENTS The authors would like to thank Margareth Ribe and Maria Ruud for their work as research coordinators.

FUNDING SUPPORT AND AUTHOR DISCLOSURES

This work was supported by the Norwegian Research Council (project 288438). Dr. Asselbergs has been supported by UCL Hospitals NIHR Biomedical Research Centre. Dr. Haugaa has licensed a patent of mechanical dispersion. All other authors have reported that they have no relationships relevant to the contents of this paper to disclose.

ADDRESS FOR CORRESPONDENCE: Prof. Kristina H. Haugaa, Department of Cardiology, Oslo University Hospital, Rikshospitalet, Sognsvannsveien 20, 0372 Oslo, Norway/P.O. Box 4950 Nydalen, 0424 Oslo, Norway. E-mail: Kristina.Haugaa@medisin.uio.no.

PERSPECTIVES

CLINICAL COMPETENCIES: The use of cascade genetic screening in AC is presenting clinicians with an expanding group of asymptomatic genotype-positive relatives with an important arrhythmic risk. Deformation imaging detects early structural and functional abnormalities indicating increased risk of VAs and may help risk stratification in early disease.

TRANSLATIONAL OUTLOOK: Deformation imaging in the easily available echocardiographic assessment has become part of daily clinical practice in many centers. We compared 2 cohorts of patients with AC from 2 different centers and externally validated 2 methods of deformation imaging. Both methods showed validity for detection of early structural and functional abnormalities, and the combination of the methods increased clinical risk stratification of patients with AC.

REFERENCES

1. Marcus FI, Fontaine GH, Guiraudon G, et al. Right ventricular dysplasia: a report of 24 adult cases. Circulation 1982;65:384–98.

2. Thiene G, Nava A, Corrado D, Rossi L, Pennelli N. Right ventricular cardiomyopathy and sudden death in young people. N Engl J Med 1988;318:129–33.

3. Corrado D, Link M, Calkins H. Arrhythmogenic right ventricular cardiomyopathy. N Engl J Med 2017;376:61–72.

4. Groeneweg JA, Bhonsale A, James CA, et al. Clinical presentation, long-term follow-up, and outcomes of 1001 arrhythmogenic right ventricular dysplasia/cardiomyopathy patients and family members. Circ Cardiovasc Genet 2015;8:437–46.

5. Marcus FI, McKenna WJ, Sherrill D, et al. Diagnosis of arrhythmogenic right ventricular cardiomyopathy/Dysplasia: Proposed modification of the task force criteria. Circulation 2010;121:1533–41.

6. Mast TP, Teske AJ, Walmsley J, et al. Right ventricular imaging and computer simulation for electromechanical substrate characterization in arrhythmogenic right ventricular cardiomyopathy. J Am Coll Cardiol 2016;68:2185–97.

7. Mast TP, Taha K, Cramer MJ, et al. The prognostic value of right ventricular deformation imaging in early arrhythmogenic right ventricular cardiomyopathy. J Am Coll Cardiol Img 2019;12:446–55.

8. Sarvari SI, Haugaa KH, Anfinsen OG, et al. Right ventricular mechanical dispersion is related to malignant arrhythmias: a study of patients with arrhythmogenic right ventricular cardiomyopathy and subclinical right ventricular dysfunction. Eur Heart J 2011;32:1089–96.

9. Leren IS, Saberniak J, Haland TF, Edvardsen T, Haugaa KH. Combination of ECG and echocardiography for identification of arrhythmic events in early ARVC. J Am Coll Cardiol Img 2017;10:503–13.

10. Lie ØH, Rootwelt-Norberg C, Dejgaard LA, et al. Prediction of life-threatening ventricular arrhythmia in patients with arrhythmogenic cardiomyopathy: a primary prevention cohort study. J Am Coll Cardiol Img 2018;11:1377–86.

11. Malik N, Win S, James CA, et al. Right ventricular strain predicts structural disease progression in patients with arrhythmogenic right ventricular cardiomyopathy. J Am Heart Assoc 2020;9:e015016.

12. Saberniak J, Leren IS, Haland TF, et al. Comparison of patients with early-phase arrhythmogenic right ventricular cardiomyopathy and right

ventricular outflow tract ventricular tachycardia. Eur Heart J Cardiovasc Imaging 2017;18:62–9.

13. Chivulescu M, Lie ØH, Popescu BA, et al. High penetrance and similar disease progression in probands and in family members with arrhythmogenic cardiomyopathy. Eur Heart J 2020;41:1401–10.

14. Peachey H, Pedersen CT, Kay GN, et al. EHRA/HRS/APHRS expert consensus on ventricular arrhythmias. Heart Rhythm 2014;11:166–96.

15. Haugaa KH, Basso C, Badano LP, et al. Comprehensive multi-modality imaging approach in arrhythmogenic cardiomyopathy-an expert consensus document of the European Association of Cardiovascular Imaging. Eur Heart J Cardiovasc Imaging 2017;18:237–53.

16. Mast TP, Teske AJ, Doevendans PA, Cramer MJ. Current and future role of echocardiography in arrhythmogenic right ventricular dysplasia/cardiomyopathy. Cardiol J 2015;22:362–74.

17. Teske AJ, De Boeck BWL, Melman PG, Sieswerda GT, Doevendans PA, Cramer MJM. Echocardiographic quantification of myocardial function using tissue deformation imaging, a guide to image acquisition and analysis using tissue Doppler and speckle tracking. Cardiovasc Ultrasound 2007;5:27.

18. Badano LP, Kolias TJ, Muraru D, et al. Standardization of left atrial, right ventricular, and right atrial deformation imaging using two-dimensional speckle tracking echocardiography: A consensus document of the EACVI/ASE/Industry Task Force to standardize deformation imaging. Eur Heart J Cardiovasc Imaging 2018;19:591–600.

19. Mast TP, Teske AJ, Te Riele AS, et al. Prolonged electromechanical interval unmasks arrhythmogenic right ventricular dysplasia/cardiomyopathy in the subclinical stage. J Cardiovasc Electrophysiol 2016;27:303–14.

20. Teske AJ, Cox MG, De Boeck BW, Doevendans PA, Hauer RN, Cramer MJ. Echocardiographic tissue deformation imaging quantifies abnormal regional right ventricular function in ARVD/C. J Am Soc Echocardiogr 2009;22:920–7.

21. Teske AJ, Cox MGPJ, Te Riele ASJM, et al. Early detection of regional functional abnormalities in asymptomatic ARVD/C gene carriers. J Am Soc Echocardiogr 2012;25:997–1006.

22. Collier P, Phelan D, Klein A. A test in context: myocardial strain measured by speckle-tracking echocardiography. J Am Coll Cardiol 2017;69:1043–56.

23. Voigt J-U, Pedrizzetti G, Lysyansky P, et al. Definitions for a common standard for 2D speckle tracking echocardiography: consensus document of the EACVI/ASE/Industry Task Force to standardize deformation imaging. J Am Soc Echocardiogr 2015;28:183–93.

24. Edvardsen T, Haugaa KH. Imaging assessment of ventricular mechanics. Heart 2011;97:1349–56.

25. Taha K, Mast TP, Cramer MJ, et al. Evaluation of disease progression in arrhythmogenic cardiomyopathy: the change of echocardiographic deformation characteristics over time. J Am Coll Cardiol Img 2020;13:631–4.

26. Claeys M, Claessen G, Claus P, et al. Right ventricular strain rate during exercise accurately identifies male athletes with right ventricular arrhythmias. Eur Heart J Cardiovasc Imaging 2020;21:282–90.

27. Te Riele AS, James CA, Philips B, et al. Mutation-positive arrhythmogenic right ventricular dysplasia/cardiomyopathy: the triangle of dysplasia displaced. J Cardiovasc Electrophysiol 2013;24:1311–20.

28. Czimbalmos C, Csecs I, Dohy Z, et al. Cardiac magnetic resonance based deformation imaging: role of feature tracking in athletes with suspected arrhythmogenic right ventricular cardiomyopathy. Int J Cardiovasc Imaging 2019;35:529–38.

29. Pieles GE, Grosse-Wortmann L, Hader M, et al. Association of echocardiographic parameters of right ventricular remodeling and myocardial performance with modified task force criteria in adolescents with arrhythmogenic right ventricular cardiomyopathy. Circ Cardiovasc Imaging 2019;12:e007693.

30. Cadrin-Tourigny J, Bosman LP, Nozza A, et al. A new prediction model for ventricular arrhythmias in arrhythmogenic right ventricular cardiomyopathy. Eur Heart J 2019;40:1850–8.

KEY WORDS arrhythmogenic cardiomyopathy, ARVC, deformation imaging, strain, ventricular arrhythmia

APPENDIX For an expanded Methods section and supplemental tables, please see the online version of this paper.